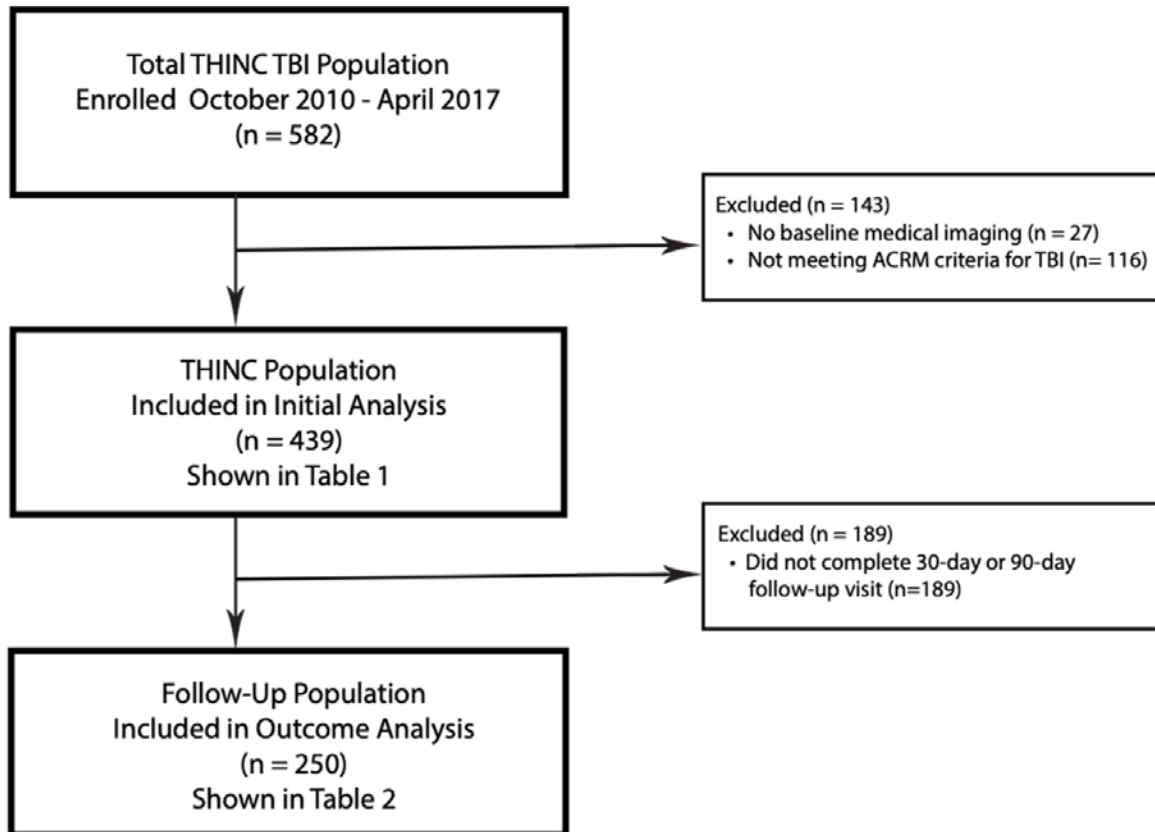


Supplemental Table 1: MRI Parameters for T2*-weighted Sequences

	MRI Parameters for T2*-weighted Sequences					
	1.5T MRI: Siemens		3T MRI: Siemens		3T MRI: Phillips	
	Short TE	Long TE	Short TE	Long TE	Short TE	Long TE
Field of View	24 cm	24 cm	22 cm	22 cm	24 cm	24cm
Repetition Time (TR)	800 ms	4300 ms	700 ms	20ms	800 ms	51 ms
Echo Time (TE)	25 ms	40 ms	12 ms	27 ms	12 ms	20 ms
Flip Angle	30°	90°	30°	15°	30°	10°
Acquisition Matrix	256 x 192	384 x 192	320 x 240	256 x 233	320 x 322	368 x 336
Scan Time	2 min	1 min	1.5 min	3.75 min	2.5 min	1.5 min

Short TE is a gradient recalled echo (GRE) sequence, while the long TE sequences are most similar to a Susceptibility Weighted Image (SWI). The long TE allows for better visualization of vessels, which is used to identify a linear TMBs from vessels.

Supplemental Figure 1: Patient Selection



Supplemental Table 2: Demographic and Clinical Characteristics of Patients With and

Demographic and Clinical Characteristics of Patients With and Without Follow-Up					
	Total (n=439)	Follow-Up (n=250)	No Follow-Up (n=189)	P-Value	χ^2 df
Demographics					
Age					
18-30	121 (28%)	56 (22%)	65 (34%)	0.006	10.253 ₂
31-64	255 (58%)	150 (60%)	105 (56%)		
65 +	63 (14%)	44 (18%)	19 (10%)		
Gender					

Without Follow-Up

Male	317 (72%)	173 (69%)	144 (76%)	0.115	4.328 ₂
Race					
White	281 (64%)	172 (69%)	109 (58%)		
African-American	122 (28%)	58 (23%)	64 (34%)	0.039	6.514 ₂
Other	36 (8%)	20 (8%)	16 (9%)		
ED Intake					
Trauma Level					
Level-1	208 (47%)	108 (43%)	100 (53%)		
Level-2	231 (53%)	142 (57%)	89 (47%)	0.053	4.070 ₁
TBI Diagnosis					
Mild	365 (83%)	211 (84%)	154 (81%)		
Moderate	55 (13%)	29 (12%)	26 (14%)	0.721	0.654 ₂
Severe	19 (4%)	10 (4%)	9 (5%)		
Clinical CT					
CT -					
Parenchymal Hemorrhage -	310 (71%)	176 (70%)	134 (71%)	0.916	0.013 ₁
Extra-Axial Hemorrhage -	385 (88%)	221 (88%)	164 (87%)	0.661	0.264 ₁
	323 (74%)	180 (72%)	143 (76%)	0.444	0.742 ₁
TMB Classification					
Presence of Any TMBs	134 (31%)	94 (38%)	40 (21%)	0.001	13.710 ₁
Presence of Punctate TMBs	108 (25%)	74 (30%)	34(18%)	0.005	7.822 ₁
No Punctate	331 (75%)	176 (71%)	155 (82%)		
<5	79 (18%)	51 (20%)	28 (15%)	0.008	9.705 ₂
≥ 5	29 (7%)	23 (9%)	6 (3%)		
Presence of Linear TMBs	90 (21%)	67 (27%)	23 (12%)	0.001	14.136 ₁
Presence of Both: Linear & Punctate	64 (15%)	47 (19%)	17 (9%)	0.004	8.310 ₁

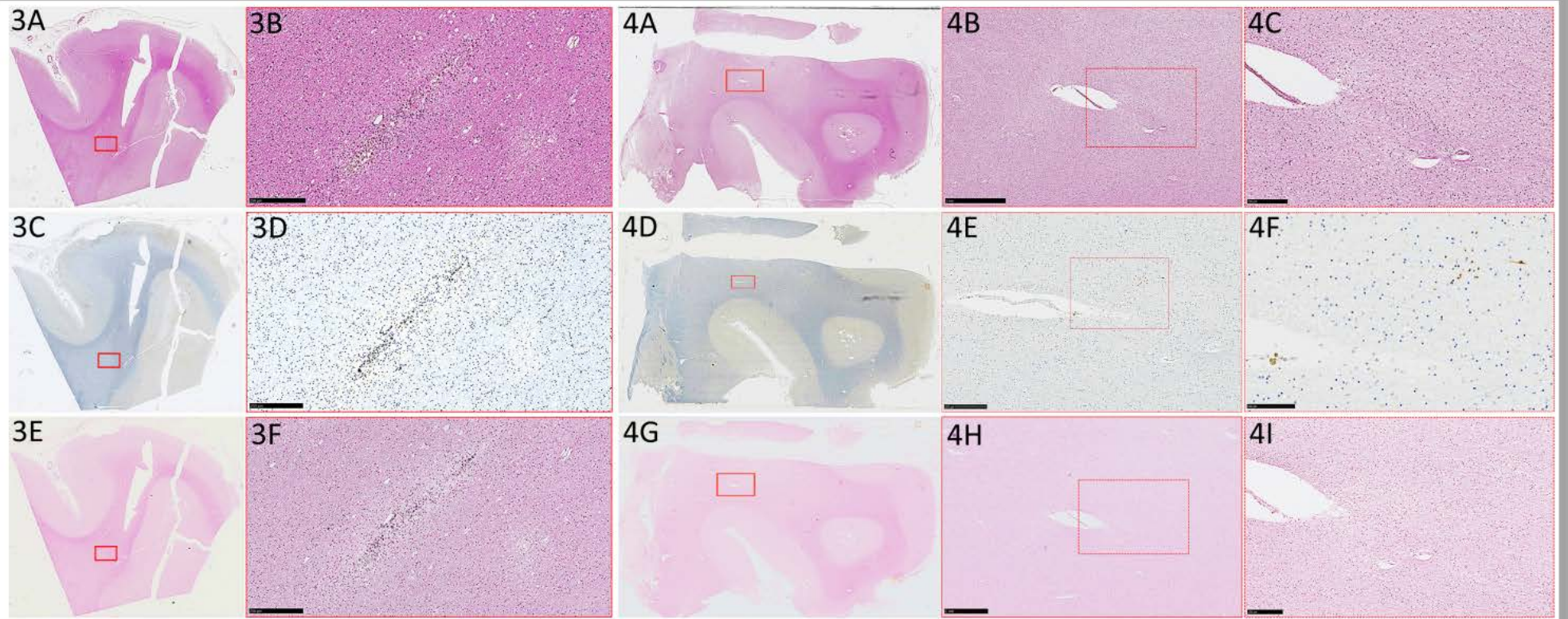
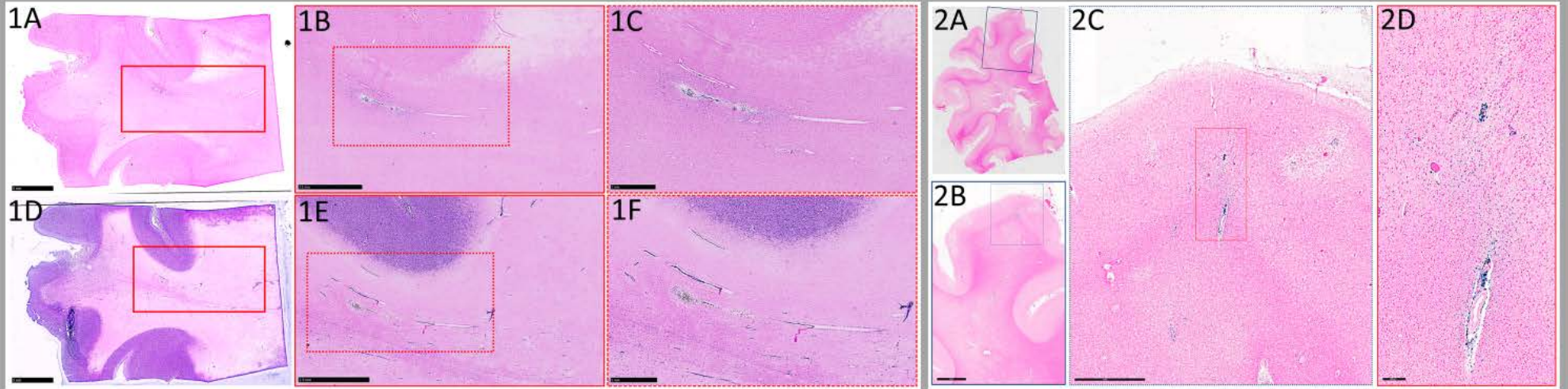
Significance (bold) was determined for any *P*-value less than 0.05.

Supplemental Table 3: Logistic Regression Analysis of Demographic and Clinical Predictors of Outcome

Logistic Regression Analysis of Demographic and Clinical Predictors of Outcome				
Predictors	Univariate Analysis		Logistic Regression	
	OR (95%)	P-Value	OR (95%)	P-Value
Trauma Level	0.280 (0.165 – 0.476)	0.001	3.140 (1.799 – 5.480)	0.001
Presence of Both: Linear & Punctate TMBs	0.398 (0.208 – 0.761)	0.005	1.423 (1.196 – 4.908)	0.014
Time from Injury to Research MRI		0.001 ^a	0.969 (0.948 – 0.989)	0.003

Hosmer-Lameshow goodness-of-fit test with $df = 8$ showed $\chi^2 = 7.407$ and $P = 0.493$

^aCalculated using nonparametric Mann-Whitney U test.



Supplemental Figure 2: Supplemental Figure 2: Distribution of Histopathology In Evaluation for Presence or Absence of Vascular and Axonal Injury.

A wide sampling of the brain was obtained and used for histopathological analysis to identify the presence or absence of vascular injury and axonal injury. (1A-C) Perls Prussian blue staining revealed large and small vessels perpendicular to cortex that were surrounded by macrophages containing iron-staining hemosiderin pigment, which is indicative of vascular injury. (1D-F) H&E staining revealed reactive astrocytosis, enlarged perivascular spaces & myelin pallor in adjacent parenchyma. We did not observe axonal dysregulation or axonal spheroids on H&E (1D-F), indicating an absence of axonal injury in this block of tissue. In large-format histopathology (2A-D) of Perls Prussian blue stain for iron, we observed a similar pattern of iron laden macrophages surrounding a large vessel. On standard H&E (3A-B) stained sections, we observed enlarged perivascular spaces, reactive astrocytosis and loss of neuropil located proximal to macrophages in the perivascular space (3B); which are characteristic of ischemia. H&E sections (3A-B) did not reveal any indications of axonal injury pathologies (i.e. no axonal dysregulation or axonal spheroids). Absence of axonal injury was confirmed on corresponding section stained with APP (3C-D); no areas of positive APP axonal processes were observed in this block of tissue. Vascular injury was identified on Perls staining (3E-F), in which a collection of Perls positive iron-laden macrophages was observed around a large vessel (3F) adjacent to ischemic regions (3A-B). In the block of tissue that was negative for TMBs on *in vivo* and *ex vivo* MRI (4A-I), we did not observe vascular injury. We did, however, observe occasional axonal injury in the corresponding APP stained section (4D-F). A small amount of APP positive axonal processes was identified in proximity to an enlarged perivascular space in the white matter (4E & 4F). In the region positive for APP (4E & 4F), no hemosiderin-laden macrophages or other pathologies suggestive of vascular injury were observed on H&E (4B and 4C) nor Perls (4H and 4I). H&E (4A-C) stained sections revealed enlarged perivascular spaces and rarefaction of the neuropil, indicating subacute to chronic ischemia. Overall, the histopathological analysis of tissue blocks that were positive for presence of TMBs on *in vivo* and *ex vivo* MRI, revealed consistent vascular injury with adjacent ischemia, resulting in loss of the surrounding parenchyma. These blocks were also consistently negative for axonal injury. While, the histopathological analysis of a tissue block that was negative for TMBs on *in vivo* and *ex vivo* MRI and negative for vascular injury, it was positive for occasional axonal injury.

This analysis includes (1A-F) tape-transfer histopathology from the left dorsal region of frontal lobe; (2A-D) large-section histology from left posterior region of frontal lobe; (3A-F) standard histopathology sections from the left parietal lobe; and (4A-I) a standard histopathology section from the basal ganglia, adjacent to the lateral ventricle. Three tissue blocks (1A-F, 2A-D and 3A-F) were co-localized to TMBs seen on *in vivo* and *ex vivo* imaging, while one tissue block (4A-I) was co-localized to a region negative for TMBs on *in vivo* and *ex vivo* imaging and used as a control. To investigate presence or absence of axonal injury and vascular injury we stained sections using Perls Prussian blue stain for iron (1A-C, 2A-D, 3E-F, 4G-I), H&E (1D-F, 3A-B, 4A-C), and APP (3C-D, 4D-F).

Solid line box (1A) indicates the enlarged region shown in 1B. Dotted red line box (1B) indicates enlarged region shown in 1C. Solid line box (1D) includes the enlarged region shown in 1E. Dotted red line box (1E) indicates enlarged region in 1F. Solid blue line box (2A) indicates enlarged region in 2B. Dotted blue box (2B) indicates enlarged region in 2C. Solid red box (2C) indicates enlarged section in 2D. Solid red box (3A, 3C and 3E) indicates enlarged region in 3B, 3D and 3F. Solid red box I (4A, 4D and 4F) indicates enlarged region in 4B, 4E and 4H. Dotted red box (4B, 4E and 4H) indicates enlarged region in 4C, 4F and 4I. Scale bars 1B & 1E = 2.5 mm; 1C, 1F, 4B, 4E & 4H = 1 mm; 2B = 5mm; 2C = 2mm; 2D = 200 μ m; 3B, 3D, 3F, 4C, 4F, & 4I = 250 μ m; 4B, 4E & 4H = 100 μ m.